IEEE Transactions on Power Delivery, Vol. 5, No. 2, April 1990

DEVELOPMENT OF OPTICAL INSTRUMENT TRANSFORMERS

T. Sawa, K. Kurosawa,
Tokyo Electric Power Company
Tokyo, Japan

T. Kaminishi, T. Yokota
Toshiba Corporation
Tokyo, Japan

Abstract – The optical instrument transformer is a current and voltage measuring system based on Faraday and Pockels effects, whose principles differ from those of conventional industrial transformers. In principle, this transformer is excellent in such aspects as control of electromagnetic induction noise, rationalization of electrical insulation, and extension of dynamic ranges and frequency bands. By making use of such excellent properties, it is possible to achieve higher performance, higher compactness, and higher reliability of instrument transformers.

This paper deals with the designing, assembling, and testing results of a prototype of an optical current transformer (CT) and that of a voltage dividing-type voltage transformer (PD). The optical CT and PD were developed to be applicable to 3-phase-enclosed-type 300kV gas-insulated switchgear (GIS) and air-insulated 168kV substation systems. Test results for the newly developed optical CT and PD showed that their basic properties conform with JEC 1201, Japanese standard for electric-power instrument transformers.

Keywords: Optical instrument transformer – CT – PT – PD – Faraday effect – Pockels effect – Workable application

INTRODUCTION

To measure currents, power plants and substations conventionally employ inductive-type CTs with cores and windings. To measure voltages, they utilize electromagnetic induction-type voltage transformers (PT) or capacitor voltage dividing-type voltage transformers (PD).

As power facilities are being developed toward higher voltages and larger capacities, machines toward higher compactness, and control and protective systems toward higher performance, there are rising demands for higher performance, higher compactness, and higher reliability of sensors or instrument transformers for detecting currents and voltages as important means of information used to assure protection and control.

On the other hand, recent progress of optical technology has been so prominent that it is expected to meet such demands by developing techniques for measuring currents and voltages by applying optical technology—in other words, by developing optical CTs and PDs.

The principle of the optical CT is to measure the magnetic field caused by a current by using optical modulation and demodulation in accordance with the Faraday effect [1]. Thus, in principle, it is possible to measure dc current, and if the material of sensor elements is not ferromagnetic, compact and lightweight CTs free of magnetic saturation can be designed. Also, the use of light for transmitting signals is advantageous for electrical insulation and control of electromagnetic induction noise. If optical CTs are developed by making use of such features, it will enable the dynamic ranges of CTs to be extended, while achieving a compact and lightweight construction of units.

The principle of the optical PD is to measure voltages by using optical modulation and demodulation in accordance with the Pockels effect [2]. With the optical PD, the input impedance into the sensor elements can be raised by reducing the size of sensor elements. This enables designing a voltage-measuring system smaller than a conventional PT by combining an optical PD with a capacitor voltage divider. Also, the optical PD is not affected by surge noise, permitting the response frequency band to be extended to a required value.

From this point of view, Tokyo Electric Power Co. and Toshiba Corp. have jointly cooperated to develop practicable optical CTs and PDs for protection and control purposes. In this development, consideration was given to the prospect and effect of application, and 300kV GIS transformers and 168kV air-insulated facilities were chosen as applicable facilities. Table I shows development targets for the optical CT and PD developed.

Table I Development targets for optical CT and PD

		GIS type	Porcelain type
Applicable equipment	Rated line voltage	300kV	168kV
		3-phase-enclosed type	–
	Rated current	4000A	2000A
	Max. current	Approx. 180kA ($2\sqrt{2}$ X 63kA)	20 kA
Target standard	Optical CT	JEC 1201 1PS + 1T class	1P class
	Optical PD	JEC 1201 1T class	–

This paper describes the principles, structures, operations, and results of tests conducted after developing the GIS-type optical CT, porcelain-type optical CT (for air-insulated transformers), and GIS-type optical PD.

OPTICAL CT

Principles

As shown in Fig. 1, the optical CT makes use of the Faraday effect. Injecting a linearly polarized light in parallel with the magnetic

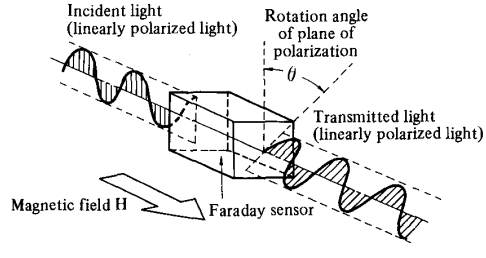

Fig. 1 Concept of Faraday effect

field H being measured to a Faraday sensor placed in the magnetic field causes the plane of polarization of outgoing light to rotate in proportion to the magnetic field. The angle of rotation θ_F, proportional to the magnetic field H impressed, is given by

$$\theta_F = VHL \quad (1)$$

where V: Verdet constant (rad/A)
H: field intensity (A/m)
L: length of light beam (m).

Thus, the field intensity or the current level can be perceived by measuring the angle of rotation θ.

89 TD 380-7 PWRD A paper recommended and approved by the IEEE Power System Instrumentation & Measurements Committee of the IEEE Power Engineering Society for presentation at the IEEE/PES 1989 Transmission and Distribution Conference, April 2 - 7, 1989. Manuscript submitted October 6, 1988; made available for printing January 26, 1989.

There are two practical methods for detecting the Faraday rotation angle: light power amplitude detection and light power phase detection.

Figure 2 shows the basic structure for amplitude detection. The beam from a light source is guided by a transmitting optical fiber to a sensor element, and then passes through a polarizer, a Faraday sensor, and an analyzer. Thus, the beam intensity-modulated in accordance

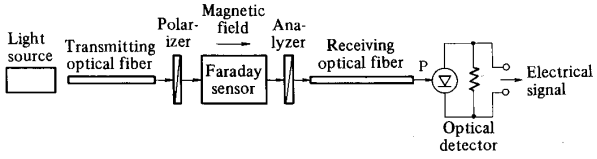

Fig. 2 Basic structure of amplitude-detection-type optical CT

with field intensity H is guided to a receiving optical fiber, and its intensity is converted into an electrical signal by a photo detector. With the power of the light source and the azimuth difference between the polarizer and the analyzer written as P_0 and 45° respectively, the intensity of output light P is given by

$$P = \alpha P_0 (1 + \sin 2\theta_F) \tag{2}$$

where α: constant ($\alpha < 1$).

Figure 3 shows the principles of light power phase detection.

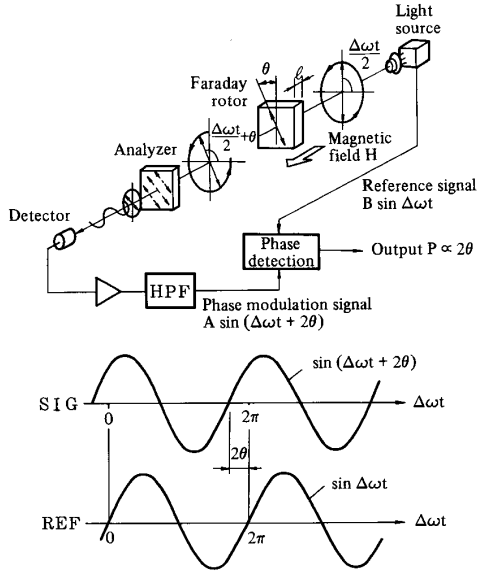

Fig. 3 Principles of light power phase detection system

Injecting a linearly polarized light with the polarization azimuth rotating at angular frequency $\Delta\omega/2$ into a Faraday sensor causes the outgoing light to become a linearly polarized rotating light with the azimuth deviated by θ_F from the incident light in accordance with the Faraday effect. When this light coming out of the analyzer is converted into an electrical signal by a photo diode, the signal P_s is a sine-wave signal phase-modulated by angle $2\theta_F$, possessing angular frequency $\Delta\omega$ as shown by

$$P_s = \alpha P_0 \{1 - \sin (\Delta\omega t + 2\theta_F)\} \tag{3}$$

Also, it is possible to choose from the light source the reference signal P_r represented by

$$P_r = \sin \Delta\omega t \tag{4}$$

Thus, the Faraday rotation angle can be perceived by choosing the ac component in equation (3) and the phase difference ϕ in equation (4), as shown below:

$$\phi = (\Delta\omega t + 2\theta_F) - \Delta\omega t = 2\theta_F \tag{5}$$

Obviously, this method enables the Faraday rotation angle θ_F to be perceived linearly in the range of $|2\theta| \leqslant 180°$.

Problems Related to Development and Methods Used

In practice, to construct an optical CT as a power unit, the Faraday sensor must be located near a high-voltage primary conductor possessing a large field produced by the current.

With this knowledge, discussions were held regarding the GIS and porcelain types, and an optical CT was designed. The types adopted after studies for major design items and the reasons for adoption are explained as follows.

a) Materials of sensor elements

Faraday-effect materials that were reviewed for sensor elements of optical CTs include ferromagnetic materials such as YIG, and crystals such as BSO and BGO, in addition to flint glass. Finally, flint glass (SF57) was chosen for the following reasons:

- Flint glass is nonmagnetic. Not only does it possess favorable temperature characteristics of the Verdet constant, but it also has a relative permeability of nearly 1, causing no disturbances in the measurement field. It produces no magnetic saturation for the magnetic field caused by a large current.
- As a glass material, it enables elements of large sizes or complicated shapes to be formed. Also highly transparent, it enables circular integral-type sensors, described later, to be made.
- The photoelastic constant of SF57 is so small that stress generation in the sensor element causes little linear birefringence in the element.

b) Site of field detection

The optical CT is based on the principles that detect the magnetic field generated around the current being measured and convert it to current. To prevent magnetic fields caused by currents of other phases, a circular integral-type sensor element, whose light beam circulates a conductor designed by directly applying the law of ampere circular integration, was employed [3]. Also, to prevent the effect—though slight—of magnetic fields of other phases caused by the existence of light beams other than closed-loop ones, the sensor element was surrounded with an aluminum magnetic shield.

c) Transmission of light

With the GIS type, for transmission in the electrically insulated space (between the GIS tank and the sensor element), a spatial transmission system in SF_6 gas was employed to ensure the reliability of electrical insulation. Since this design threatened stability of the received light power with respect to GCB vibration and temperature variations, an insulating cylinder was used to hold the sensor, and a light power phase detection system was employed for signal detection, as described in paragraphs d) and e) below.

With the porcelain type, transmission through optical fiber was also used in the porcelain tube, an electrically insulated space. This design was used because the porcelain tube was longer than the length of electrical insulation in the GIS type, assuring insulation reliability even with the use of optical-fiber transmission. The porcelain tube was filled with SF_6 gas.

d) Securing the sensor element

To secure the sensor element near the conductor in the GIS type, the method using an insulating cylinder was finally chosen, intended—for example—to control variations in received light power caused by optical axis variations during GCB vibration, to prevent staining of optical parts with decomposed substances of SF_6 and noise caused by arc light resulting from dielectric breakdowns, to

ensure a design that would prevent direct transfer to the sensor element of Joule heat generated in the conductor, and so on. Also, the optical head containing transmitting and receiving optical fibers, lenses, a polarizer, an analyzer, and others was secured to the GIS tank side of the insulating cylinder.

With the porcelain type, an optical-fiber transmission system was used for transmission in the electrically insulated space. Thus, the optical head was integrated with the sensor element. To prevent the direct transfer of Joule heat and vibration generated in the conductor, the sensor element was attached to the cap at the top of the porcelain tube.

e) Signal detection system

As described previously, signal detection systems can be roughly classified into two types: light power amplitude detection and light power phase detection. The light power phase detection system offers the following features:

- Excellent linearity of characteristics, permitting a wide dynamic range to be obtained.
- Easy control of errors and noise resulting from variations in received light power caused by various reasons.

In the light power amplitude detection system, construction is simple.

For the up-to-300kV rated voltage type, considering that a dynamic range to cover a large current range up to 180kA (crest) was necessary and that a spatial light transmission system was used, a new light power phase detection system was developed and employed.

For the 168kV and 72kV rated voltage types, a light power amplitude detection system was used because their dynamic range was not as wide as that of the higher rated voltage type.

GIS-type Optical CT

Structure and Operations: Figure 4 shows structure of the GIS-type optical CT. Its operations, described along the light transmission

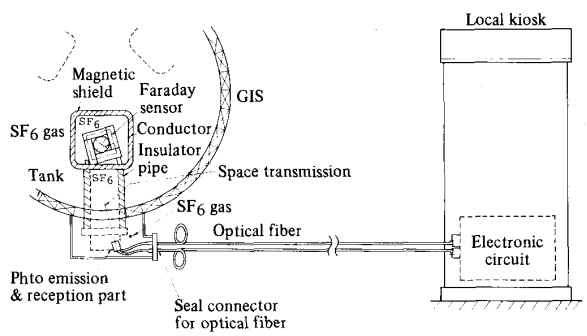

Fig. 4 Structure of GIS-type optical CT

line, are as follows. The light of the LED (wavelength: 0.85μm) mounted on the local kiosk is guided to the optical head located on the ground potential side of the insulation pipe secured to the GIS tank through a transmitting optical fiber (quartz fiber, core dia. 50μm, GI type). The optical head houses optical parts such as a polarizer, an analyzer, and lenses. Collimated by the optical head and passed through the polarizer to obtain a proper azimuth, the light is spatially transmitted within the SF_6 gas (pressure: 4 kgf/cm^2) in the insulation pipe, and then guided to the flint-glass Faraday sensor provided around the conductor. The light rotates once in each opposite direction, totaling 2 rotations around the conductor in the Faraday sensor, is subjected to Faraday rotation proportional to the current through the conductor, returns to the optical head, and enters the receiving optical fiber (multicomponent glass fiber, core dia. 400μm, SI type). Guided back to the local kiosk through the receiving optical fiber, the light is converted into an electrical signal by a photo diode (APD), and further converted into an analog output signal by a phase detection circuit.

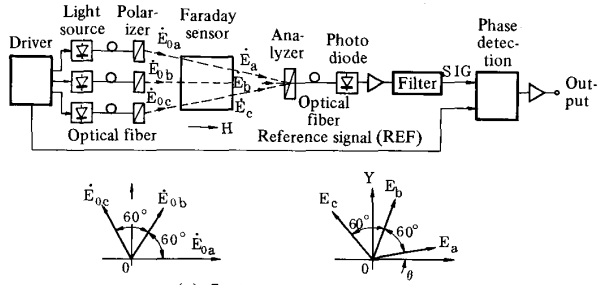

(a) System structure

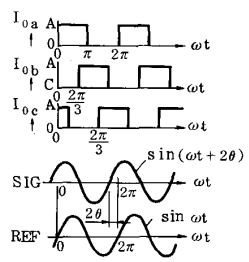

(b) Principles of phase detection

Fig. 5 Principles of light power phase detection system using 3 light sources

Figure 5 shows operations for light modulation and demodulation (phase detection) in accordance with the Faraday effect. Here, the incident light entering the Faraday sensor is linearly polarized light (rotating rate: 40 X 10^3 rotations/s) with the polarization azimuth rotating at a constant rate ω. The rotating linearly polarized light is simulated by 3 linearly polarized beams E_{0a}, E_{0b} and E_{0c} of equal light intensity, but with the planes of polarization staggered by 60°, whose beams are turned on and off with phases staggered by a 120° electrical angle. Injecting linearly polarized beams E_{0a}, E_{0b} and E_{0c} into the Faraday sensor and impressing a magnetic field H produces the outgoing light from the Faraday sensor equal to linearly polarized beams E_a, E_b and E_c, given a Faraday rotation by θ_F in proportion to the magnetic field H. With the intensities of the light sources written as I_{0a}, I_{0b} and I_{0c}, and with the analyzer azimuth set on the polarizer azimuth in the a phase, intensities I_a, I_b and I_c of the three beams passed through the analyzer are given by

$$\begin{aligned} I_a &= I_{0a}\cdot(1+\cos 2\theta_F)/2 \\ I_b &= I_{0b}/2\cdot\{1+\cos(\pi/3+2\theta_F)\} \\ I_c &= I_{0c}/2\cdot\{1+\cos(2\pi/3+2\theta_F)\} \end{aligned} \tag{6}$$

The photo diode synthesizes these three beams and outputs an electrical signal I_s represented by

$$I_s = I_a + I_b + I_c \tag{7}$$

On the other hand, I_{0a}, I_{0b} and I_{0c}, rectangular waves as shown in Fig. 5 (b), are turned on and off at a constant cycle with an intensity of A. By effecting Fourier development after inserting equation (6) into equation (7), I_s can be given by

$$I_s = \frac{3}{2}A + \frac{2A}{\pi}\left\{\frac{3}{2}\sin(\Delta\omega t + 2\theta_F) + \sin 3\Delta\omega t + \cdots\right\} \tag{8}$$

By extracting only the basic frequency component $\Delta\omega$ through filtering the photo diode output I_s, the following filter output SIG is obtainable–

$$SIG \propto (3A/\pi)\sin(\Delta\omega t + 2\theta_F) \tag{9}$$

On the other hand, from the drive circuit of the light source, the

following reference signal REF can be derived–

$$REF \propto \sin \Delta\omega t \tag{10}$$

Then, output ϕ proportional to the Faraday rotation angle θ_F shown in equation (5) can be obtained by comparing the phase differences between equations (9) and (10). To detect the phase difference ϕ, the time lag between the points when two signals SIG and REF reach the zero level is measured with a clock. Also, the system is designed to be capable of current measurement by using a carrying circuit even with $|2\theta_F|$ above 180°. The ultimate output is obtained as an analog output by passing the measured phase difference through a D/A conversion circuit.

Figure 6 shows the internal structure of the GIS-type optical CT.

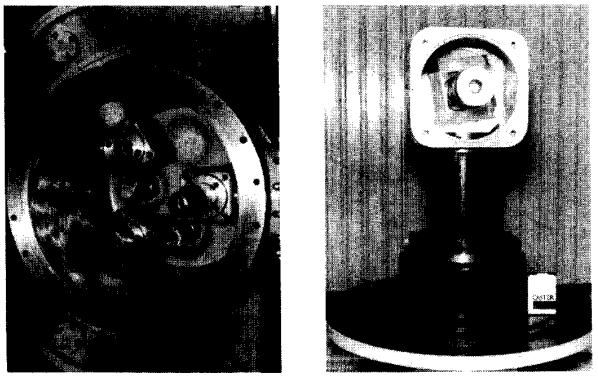

(a) Internal structure (b) Component in optical CT (for 1 phase)

Fig. 6 Internal structure of optical CT

Test Results: As shown below, basic properties of the model conform with JEC 1201 requirements.

a) Ratio error and phase displacement characteristics
With a primary current of 50Hz between 0.2 kArms and 4 kArms, rated current, ratio error and phase displacement characteristics were measured by comparing them with those of the standard CT. As shown in Fig. 7, the results well meet the standards.

b) Temperature characteristics
When the main unit and the electronic circuit of the optical CT placed in a thermostat oven reached the specified temperature, a primary current between 0.2 kArms and 1 kArms was fed, and the ratio errors and the phase displacements were measured. For the temperature range from -16°C to 40°C, ratio error variations were within ±1%, and there were no phase displacement variations.

c) Transient characteristics
With 10 cycles of a 63 kArms transient primary current (primary time constant: 0.1s, 100% dc component superimposed), the output waveforms and transient errors of the optical CT were measured. Figure 8 shows the measured waveforms. Evidently, the optical CT output is not saturated. The transient error is 7.6%, which meets the requirement of 10% or less.

Porcelain-type Optical CT

Structure and Operations: Figure 9 shows the structure of the porcelain-type optical CT. Light from the LED source (λ = 0.85μm) is guided through a transmitting optical fiber (quartz, core dia. 50μm, GI type) to a sensor element provided around the conductor. At the sensor element, the light is passed through a polarizer for linear polarization and then transferred to a Faraday sensor (circular integral type, circuiting cycle: 1). There the light is given a Faraday rotation proportional to the current through the conductor, guided to an analyzer with the azimuth turned by 45°, and converted into an optical intensity signal. The light converted into an intensity signal is guided through a receiving optical fiber (multicomponent glass, core dia. 400μm, SI type) to a photo diode and converted into an electical signal. To remove drifts from output P of the photo diode, the signal is treated as follows: signal P is divided into two, and one half is passed through a low-pass filter to obtain the mean X of the signal. Output V is obtained by using the mean X and the photo diode output P in calculation of following equation:

$$V = (P - X)/X \tag{11}$$

Figure 10 shows a photograph of the porcelain-type optical CT.

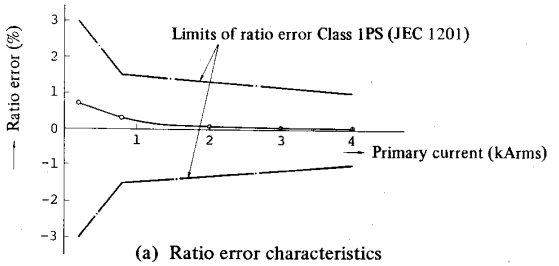

(a) Ratio error characteristics

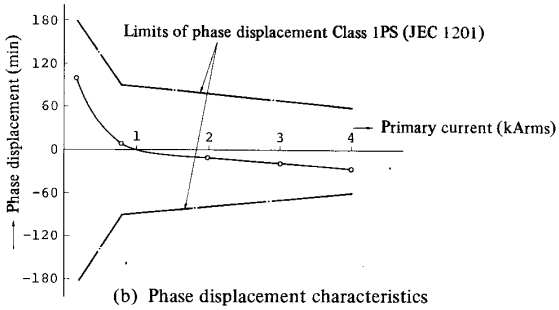

(b) Phase displacement characteristics

Fig. 7 Test for ratio error and phase displacement characteristics

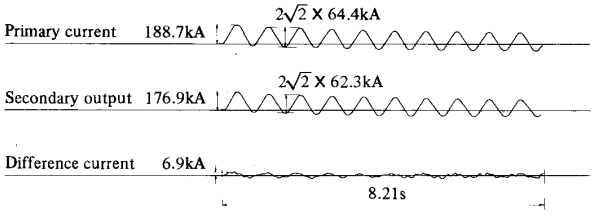

Fig. 8 Test for transient characteristics

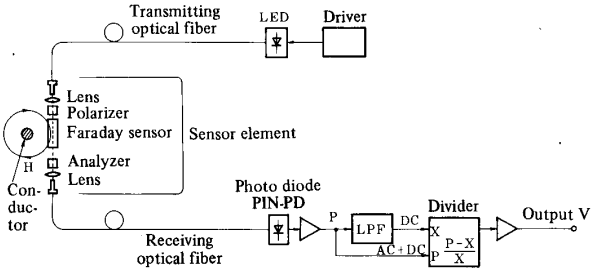

Fig. 9 Structure of porcelain-type optical CT

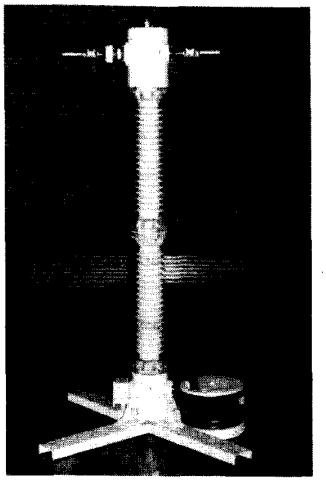

Fig. 10 Appearance of porcelain-type optical CT

Test Results: As shown below, the basic properties complied with JEC 1201 requirements.

a) Ratio error and phase displacement characteristics
With a current of 50Hz varied from 100 Arms to rated 2000A fed to the conductor, ratio errors and phase displacements were measured in comparison with the standard CT.
Figure 11 shows the test results. It is evident that the ratio errors and the phase displacements comply with the JEC 1201 standard.

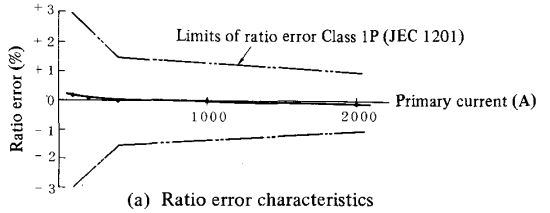

(a) Ratio error characteristics

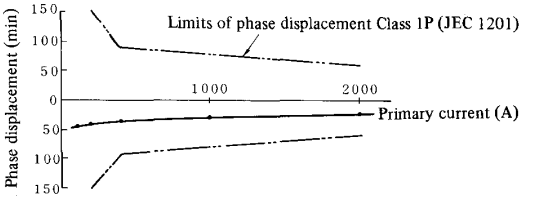

(b) Phase displacement characteristics

Fig. 11 Ratio error and phase displacement characteristics of porcelain-type optical CT

b) Temperature characteristics
The optical CT body was placed in a thermostat oven and the temperature was varied from -16°C to 40°C. When the specified temperature was reached, the ratio error and the phase displacement for a primary current 1000 Arms were measured. Ratio error variations were within ±0.4%. There were no phase displacement variations.

c) Withstand voltage limit test
To prove insulation performance primarily of the optical fiber cord in the porcelain tube, withstand voltage limit tests were conducted. In commercial-frequency withstand voltage limit tests, voltage 150% (488 kVrms) that of the test voltage specified by JEC 1201 was applied for 1 min, and there occurred no dielectric breakdown. In lightning impulse voltage withstand tests, 175% (1313kV crest) that of the test voltage specified in JEC 1201 was applied, causing no dielectric breakdown. When 180% of the specified voltage was applied, a flashover occurred on the porcelain tube surface, but without damage to the optical fiber.
This proved that dielectric strength of the optical fiber cord in the porcelain tube of the porcelain-type CT model manufactured was higher than that of the porcelain tube surface.

OPTICAL PD (FOR GIS)

Principles

As shown in Fig. 12, the optical PD is used to measure voltages by making use of the Pockels effect. Injecting a linearly polarized

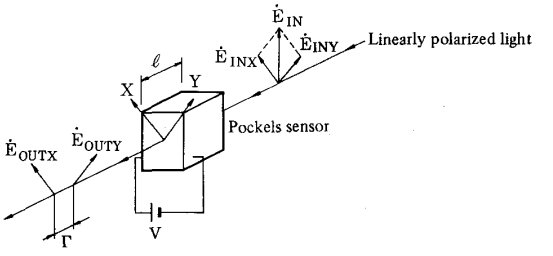

(a) Conceptual drawing of Pockels effect

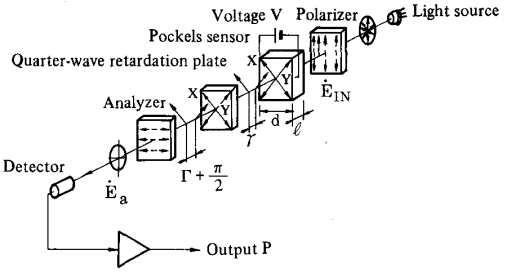

(b) Voltage measurement by light power amplitude detection system

Fig. 12 Principles of optical PD

beam E_{IN} into a Pockels sensor, to which voltage V is applied, causes the beam to be divided into 2 linearly polarized beams E_X and E_Y at different speeds and crossing each other at right angles, becoming an elliptically polarized beam resulting from a phase difference between them at the sensor outlet. This phase difference is proportional to the product of the voltage applied, the Pockels constant, and length of the element. Thus, the voltage applied can be perceived by measuring the phase difference. Similarly to the optical CT, the same methods are employed for measuring phase differences: light power amplitude detection and light power phase detection. (b) shows the structure for light power amplitude detection. The light turned into a linearly polarized beam by a polarizer is injected into a Pockels sensor at a 45° angle to the crystal axes (X, Y) of the sensor. In the Pockels sensor, the light is given a phase difference γ by voltage application. Then the emitted light is passed through a quarter-wave retardation plate to be given a 90° optical bias, and further passed through an analyzer with the azimuth turned by 90° to be converted into an intensity signal P represented by

$$P = P_0 (1 + \sin \delta) \quad (12\text{-a})$$
$$\gamma = \pi (V/V_\pi) \quad (12\text{-b})$$

where P_0: intensity of incident light into polarizer
V_π: half-wave voltage

Problems Related to Development and Methods Used

The methods chosen for the main design items with the GIS-type optical PD and reasons for their selection are explained as follows.

a) Material of sensor elements
For the material of the sensor elements, lithium niobate $LiNbO_3$, a uniaxial crystal, was chosen for the following reasons:
- Large Pockels constant and high sensitivity.
- A horizontal modulation system is permissible, enabling sensitivity to be adjusted in accordance with crystal dimensions.

In addition, $LiNbO_3$ possesses a pyro-electricity effect, which was eliminated by providing the crystals with short-circuiting electrodes. Also, uniaxial crystals involve peculiar temperature characteristics due to natural birefringence. Their effects were also eliminated by bringing together the optical axis of crystal-transmitted light and the optical axis of the crystal.

b) Location of optical voltage sensor
Possible location for the optical voltage sensor may be the high-voltage part (near the conductor in the GIS tank) or the ground potential side (the GIS tank exterior). Voltage data, unlike magnetic fields generated by currents, can be easily chosen by using a capacitor voltage divider. Thus, with a view to easing maintenance, the ground potential side was chosen.

c) Capacitor voltage divider
The optical PD model manufactured was designed for 3-phase-enclosed-type GISs. To prevent influences caused by the effect of electrical fields in other phases, electrostatic shields were formed by providing each phase with a grounding electrode.

d) Transmission of light
Since it was not necessary to transmit light in electrically-insulated spaces, only the optical-fiber transmission was adopted.

e) Signal detection system
In voltage measurement, linear characteristics of the measuring system are needed only in the measurement range from 2% to about $\sqrt{3}$ of the rating, not requiring such a wide dynamic range as that for CT. Thus, the light power amplitude detection system, requiring a simple construction, was chosen.

Structure and Operations

Figure 13 shows structure of the optical PD. The beam from the light source (LED, $\lambda = 0.85\mu m$) installed on the local kiosk is guided through a transmitting optical fiber (quartz, core dia. $50\mu m$, GI type) to the optical voltage sensor located near the GIS tank. A voltage,

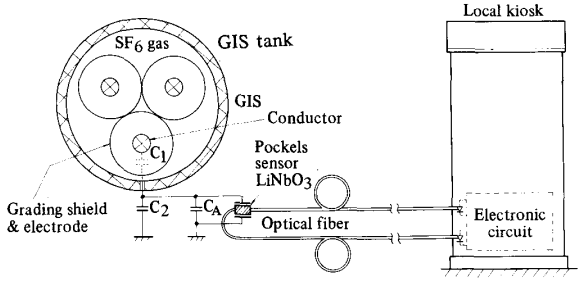

Fig. 13 Structure of optical PD

capacitor-divided from the voltage of the high-voltage conductor, is applied to the optical voltage sensor. The light with a voltage applied and intensity modulated in accordance with the Pockels effect is guided through a receiving optical fiber (multicomponent glass, core dia. $200\mu m$, SI type) to the photo diode on the field panel, and is converted into an electrical signal.

There are intermediate and grounding electrodes coaxial with the high-voltage conductor. The electrostatic capacitance between the high-voltage conductor and the intermediate electrode is determined as capacitor C_1 on the high-voltage side, and the electrostatic capacitance between the intermediate electrode and the grounding electrode is determined as capacitor C_2 on the low-voltage side. The intermediate electrode potential was drawn out of the GIS tank, and capacitor C_A is added appropriately in parallel with C_2 so that the voltage component on the low-voltage side will be $100/\sqrt{3}$V when the rated voltage is applied.

The phase difference caused in accordance with the Pockels effect in the optical voltage sensor is about 7.2 degrees (peak) for the rated voltage. The input electrostatic capacitance of the optical voltage sensor is about 17pF.

Figure 14 shows the structure of the optical voltage sensor.

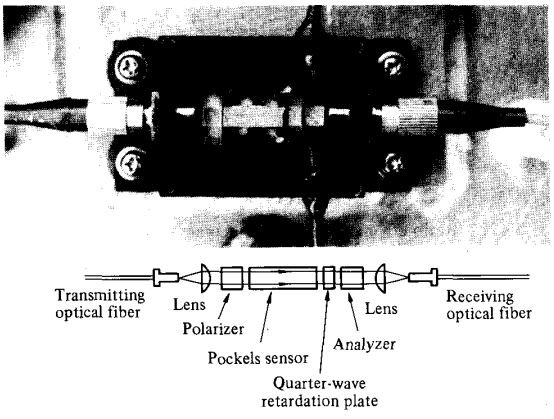

Fig. 14 Optical voltage sensor

Test Results

As shown below, the basic properties conform to JEC 1201 requirements.

a) Ratio error and phase displacement characteristics
Ratio error and phase displacement characteristics in the voltage range from 2% to 110% of the rated voltage were measured, and results comply with the JEC 1201 standard as shown in Fig. 15.

b) Temperature characteristics
The case temperature of the optical voltage sensor was varied from -20°C to 60°C, -20°C, and 60°C consecutively. Variation rates were 1.0 to 1.3 deg/min. With this temperature variation, ratio error variations for the rated voltage were within ±1% during temperature variation and within ±0.3% at a constant temperature, as shown in Fig. 16.

c) Frequency characteristics
While the frequency was varied from 47.5Hz to 52.5Hz with the rated voltage $275/\sqrt{3}$kV applied, ratio errors and phase displacements were measured. The ratio error variation was 0.05% and the phase displacement consistently remained at 1 min. These values sufficiently satisfy the requirements.

EFFECTS

Effects produced when the newly developed optical CT and PD are applied can be summarized as follows:

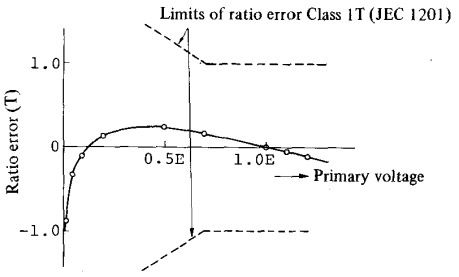

(a) Ratio error characteristics

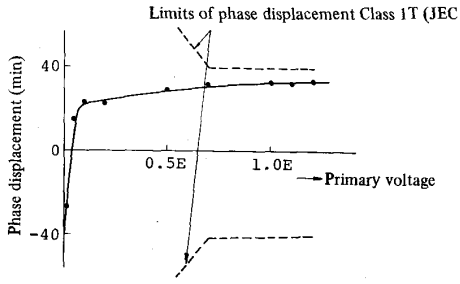

(b) Phase displacement characteristics

Fig. 15 Ratio error and phase displacement characteristics

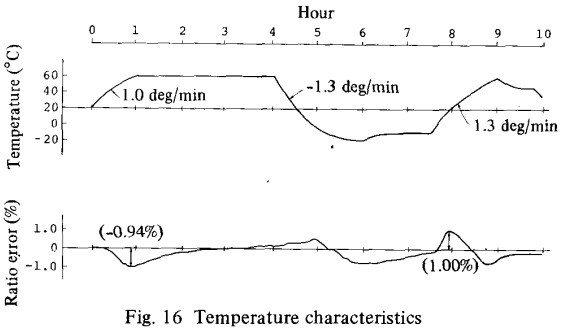

Fig. 16 Temperature characteristics

a) Optical CT
   1) Higher compactness and lighter weight—
      because no cores are necessary and insulation can be rationalized.
   2) Higher measuring performance—
      because no magnetic saturation occurs.
      - No saturation regarding large currents
      - No saturation regarding current with large dc component time constants

b) Optical PD
   1) Higher compactness—
      mainly attributable to high input impedance of the optical voltage sensor.
   2) No effect from surge noise
   3) Free selection of response frequency bands

LONG-TERM CONDUCTION TEST

The newly developed GIS-type optical CT and PD are under a long-term factory conduction test that started in August 1987 and will end in March 1989. At present, they are operating well. Figure 17 shows the entire long-term conduction test system.

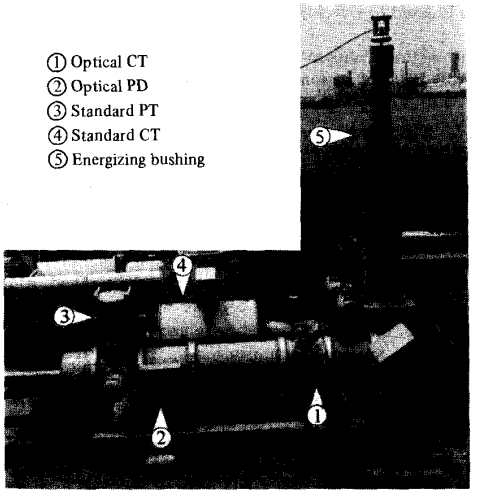

Fig. 17 300kV GIS type long-term conduction test system

CONCLUSIONS

Designing and manufacturing of the optical CT and PD newly developed for practical use have been described together with test results. These models are designed for 3-phase-enclosed-type 300kV GISs and air-insulated 168kV substation systems.

For the Faraday sensor element of the optical CT, a circular integral type made of flint glass was used to prevent influences caused by magnetic fields of other phases. For light transmission between the GIS tank and the sensor element of the GIS-type optical CT, a spatial transmission system in SF_6 gas was adopted to ensure reliability of the electrical insulation. For signal detection, a light power phase detection system was employed because it permits easy control of errors and noise resulting from luminous energy variations and also permits a wide dynamic range to be used.

For light transmission in the charger of the porcelain-type optical CT, an optical fiber in a porcelain tube filled with SF_6 gas was used. The signal detection was a light power amplitude detection type.

The GIS-type optical PD was designed to obtain the intermediate voltage by using the capacitor component with an optical voltage sensor placed on the ground side.

The developed optical CT and PD models were tested. Their basic properties comply with JEC 1201, Japanese standard for electric-power instrument transformers.

GIS-type optical CT and PD models are under a long-term factory conduction test and thus far they have been operating well.

Further, plans are being made to conduct commercial field tests to prove practical performance.

REFERENCES

[1] S. Saito et al., "Development of the Laser Current Transformer for Extra-High-Voltage Transmission Lines," IEEE Journal of Quantum Electronics, vol. QE-2, No. 8, August 1966.

[2] S. Saito et al., "Fundamental Researches on Measurements of Electric Current and Voltage in Power System by Using Laser Light," Report of The Institute of Industrial Science, The University of Tokyo, vol. 28, No. 5, March 1980.

[3] A. Hashimoto et al., "Portable Optical Current Transformer," National Meeting of The Institute of Electrical Engineers of Japan, No. 1293, 1982 (in Japanese).

[4] Y. Kuroda et al., "Field Test of Fiber-Optic Voltage and Current Sensors Applied to Gas Insulated Substation," 2nd International Technical Symposium on Optical and Electro-Optical Applied Science and Engineering, November 1985.

[5] M. Kanoi et al., "Optical Voltage and Current Measuring System for Electric Power Systems," IEEE Transactions on Power Delivery, vol. PWRD-1, No. 1, January 1986.

Takeshi Sawa was born in Ishikawa Prefecture, Japan on October 28, 1942.

In 1961, he joined Tokyo Electric Power Co., Inc. (TEPCO), Tokyo. He engaged in designing of the HVDC converter substation, 500kV substations and R&D of gas-insulated switchgear (GIS). Recently he has been working as a Senior Engineer, responsible for R&D of static var compensators (SVCs) in the Engineering Research Center of TEPCO.

Mr. Sawa is a member of the Institute of Electrical Engineers of Japan (IEEJ), and he was awarded a prize from IEEJ for the advanced development of SVCs, in 1988.

Kiyoshi Kurosawa was born in Nagano Prefecture, Japan on September 6, 1952. He received his B.S. degree in electrical engineering from Nihon University, Tokyo, in 1978 and graduated from the Department of Technology, University Course, Tokyo Electric Power Institute, Tokyo, in 1980.

In 1971, he joined Tokyo Electric Power Co., Inc., Tokyo, and since then has been engaged in R&D of optical sensors for electric power systems.

Mr. Kurosawa is a member of the Institute of Electrical Engineers of Japan and the Japan Society of Applied Physics.

Tohru Kaminishi was born in Fukuoka, Japan on September 8, 1948. He received his B.S. degree in electrical engineering from Nagasaki University, Japan, in 1971.

In 1971, he joined Toshiba Corporation. Since then, he has been engaged in research and development on instrument transformers.

Mr. Kaminishi is a member of the Institute of Electrical Engineers of Japan, the Institute of Electronics, Information and Communication Engineers of Japan, and the Japan Society of Applied Physics.

Takeshi Yokota was born in Tokyo, Japan on February 15, 1958. He received his B.S. and M.S. degrees in electrical engineering from Yokohama National University in 1980 and 1982 respectively.

In 1982, he joined Toshiba Corporation. Since then, he has been engaged in development of substation equipment such as gas-insulated switchgear and power transformers.

Mr. Yokota is a member of the Institute of Electrical Engineers of Japan.